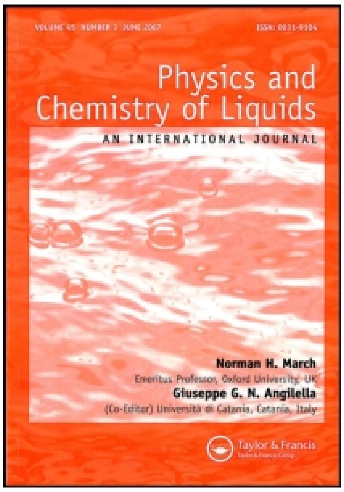

Physics and Chemistry of Liquids

Publication details, including instructions for authors and subscription information:
http://www.informaworld.com/smpp/title~content=t713646857

Dielectric relaxation study of $AgTlSe_2$ in the solid and liquid states

A. H. Abou[a]; Ela N. Abdelmohsen[a]
[a] Physics Department, Islamic Girls College, Nasr City, Cairo

To cite this Article Abou, A. H. and Abdelmohsen, Ela N.(1982) 'Dielectric relaxation study of $AgTlSe_2$ in the solid and liquid states', Physics and Chemistry of Liquids, 12: 1, 17 — 30

To link to this Article: DOI: 10.1080/00319108208084538

URL: http://dx.doi.org/10.1080/00319108208084538

Phys. Chem. Liq., 1982, Vol. 12, pp. 17-30
0031-9104/82/1201-0017$06.50/0

Printed in the U.S.A.

Dielectric Relaxation Study of $AgTlSe_2$ in the Solid and Liquid States

A. H. ABOU EL ELA and N. ABDELMOHSEN
Physics Department, Islamic Girls College, Nasr City, Cairo

(Received October 19, 1981)

Measurements of the dielectric properties of $AgTlSe_2$ in the solid and liquid states were carried out in a wide range of frequencies (10^{-2} to 10^6 Hz) at different temperatures (150°C to 600°C). The material displayed dielectric dispersion and two loss peaks were observed. The curves: $\log \varepsilon'$ vs. temperature and $\tan \delta, \varepsilon'$ vs. frequency gave a direct evidence of the existence of a Debye-type relaxation having a wide distribution of relaxation times. Cole–Cole diagrams have been used to determine the distribution parameter (α) and the molecular relaxation time (τ), and Eyring's relaxation rate equations have been used to determine the free energy of activation.

The high frequency loss peak was ascribed to charge defect $D^+ - D^-$ states and the density of states was calculated using Elliott's theory for ac conductivity and dielectric loss in chalcogenide glasses.

1 INTRODUCTION

Various models have been proposed to explain the conductivity behaviour of amorphous and liquid semiconductors,[1–4], and it has been demonstrated the some semiconductors retain their predominantly covalent semiconducting properties in the amorphous and liquid states, whereas other semiconductors acquire metallic properties above the melting point. However, no systematic efforts have so far been made to study the dielectric relaxation mechanisms of these compounds in the solid and liquid states.

The aim of the present work is to investigate the dielectric properties of $AgTlSe_2$ ternary semiconductor in the solid and liquid states. $AgTlSe_2$

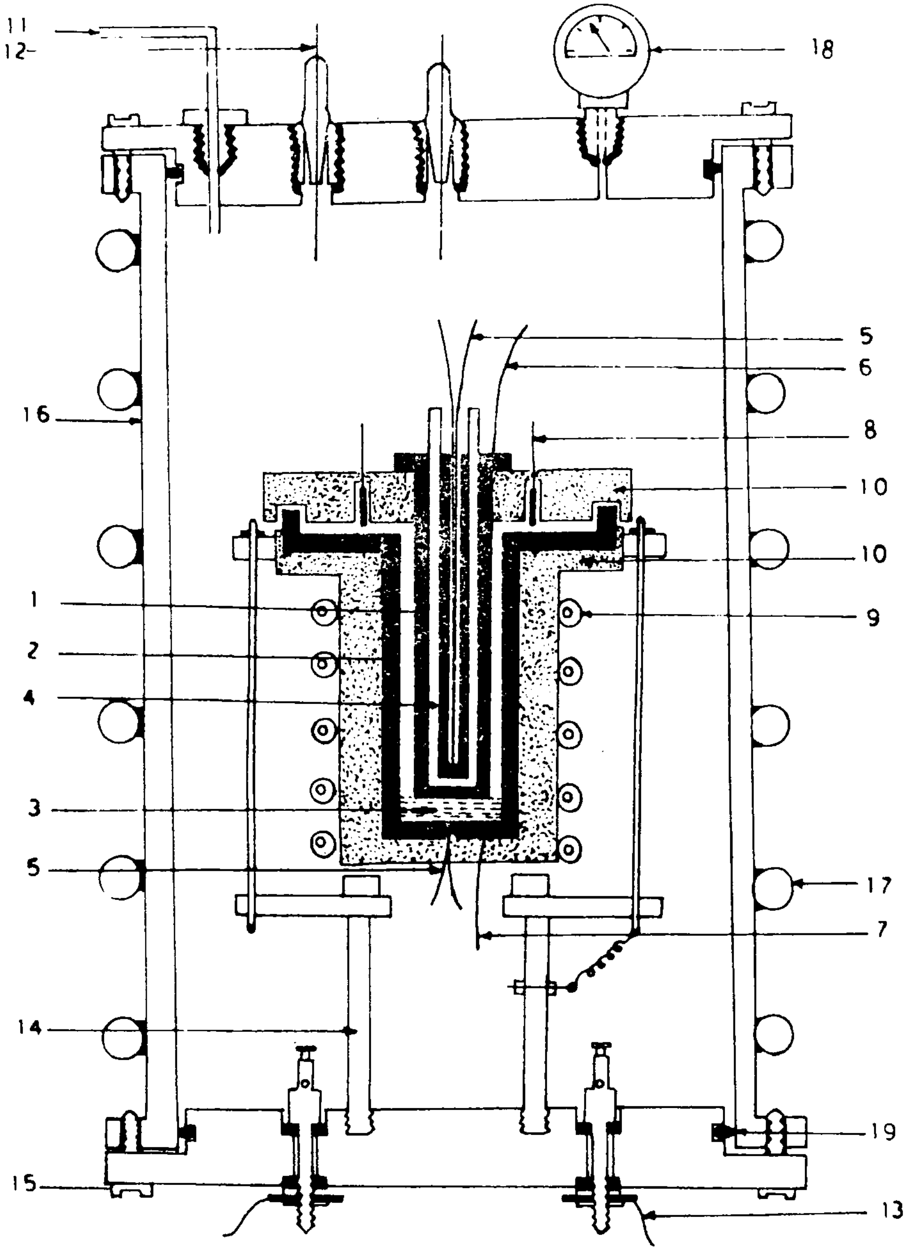

FIGURE 1 Cell holder: 1. Inner graphite electrode. 2. Outer graphite electrode. 3. Sample. 4. Aluminium radiator. 5. Thermocouples. 6, 7. Leads. 8. Guard ring electrode. 9. Heater. 10. Ceramic tube. 11. Nitrogen gas inlet. 12. Insulated connecting plugs. 13. Insulated connecting pins. 14. Cell holder. 15. Joining rivets. 16. Iron cylinder. 17. Copper tubing for cooling. 18. Pressure manometer. 19. Rubber O-sealing.

possesses the chalcopyrite structure[5,6] and its melting point is 328°C. Ternary chalcopyright semiconductors have attracted recently a greal deal of attention because of their peculiar non-linear optical properties.

The samples were prepared by melting the proper amounts of highly pure component elements (99.999%). The material was sealed in a quartz tube at 10^{-3} Pa and heated at 1200°C for 12 h with frequent rocking to ensure homogenization of the melt. Then the tubes were quenched in ice to obtain the sample in the amorphous state. The solid material is then heated in inert atmosphere until it melts and then transferred to the measuring cell.

A cylindrical measuring cell was used (Figure 1) which consists of two concentric graphite cylinders with 10^{-4} m spacing. The cell contains a temperature controlled heater, a chromel-alumel thermocouple for accurate measurements of temperature and was fitted with a guard ring electrode.

Measurements of the dielectric constants were carried out in an inert atmosphere at different frequencies and temperatures using a well shielded ac bridge according to the Schering-principle in conjunction with a Farnell ESG2 oscillator, and a sensitive broad band oscilloscope type Trio CS-1560A was used as a null indicator. Measurements in the low frequency range (from 10^{-3} Hz to 100 Hz) were carried out using a low frequency oscillator based on 1C 8038 precision waveform generator.

Electrodes were applied in various ways to see whether contacts affected the measurements and the data were found to be reproducible to better than 2%. Moreover, the results have revealed that the type of the electrode material did not play a substantial role.

3 THEORY OF MEASUREMENTS AND EXPERIMENTAL RESULTS

Figures 2 and 3 show the frequency dependence of the real part of the dielectric constant ε' and dielectric loss $\tan \delta$ at different temperatures. All curves displayed two dielectric dispersion peaks in the low frequency and high frequency ranges and the frequency at the peak maximum shifts towards higher frequencies on increasing the temperature. Moreover, the height of the loss peak $(\tan \delta)_{max}$ increases with the temperature.

(a) Distribution parameter (α) and relaxation time (τ)

Cole and Cole[7] showed that if a dielectric system has a distribution of relaxation times then the complex plane locus, obtained by plotting ε'' versus ε', is generally an arc of a circle intersecting the abscissa axis at the

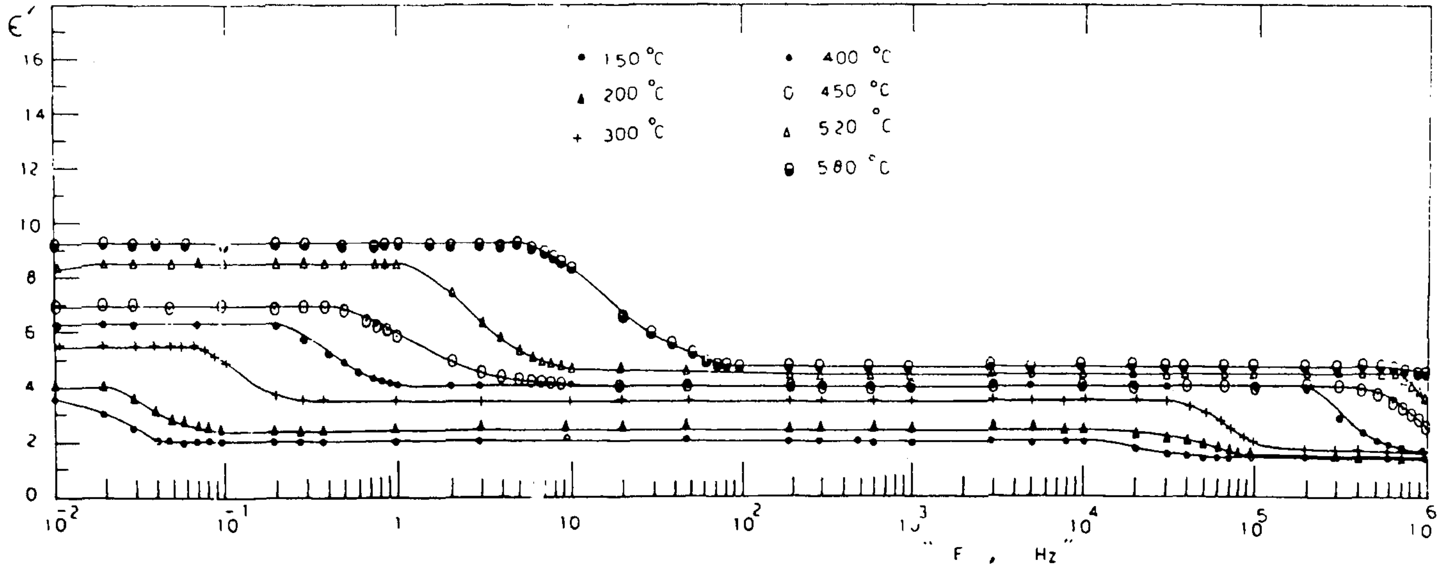

FIGURE 2 The frequency dependence of the real part of the dielectric constant ε' at different temperatures.

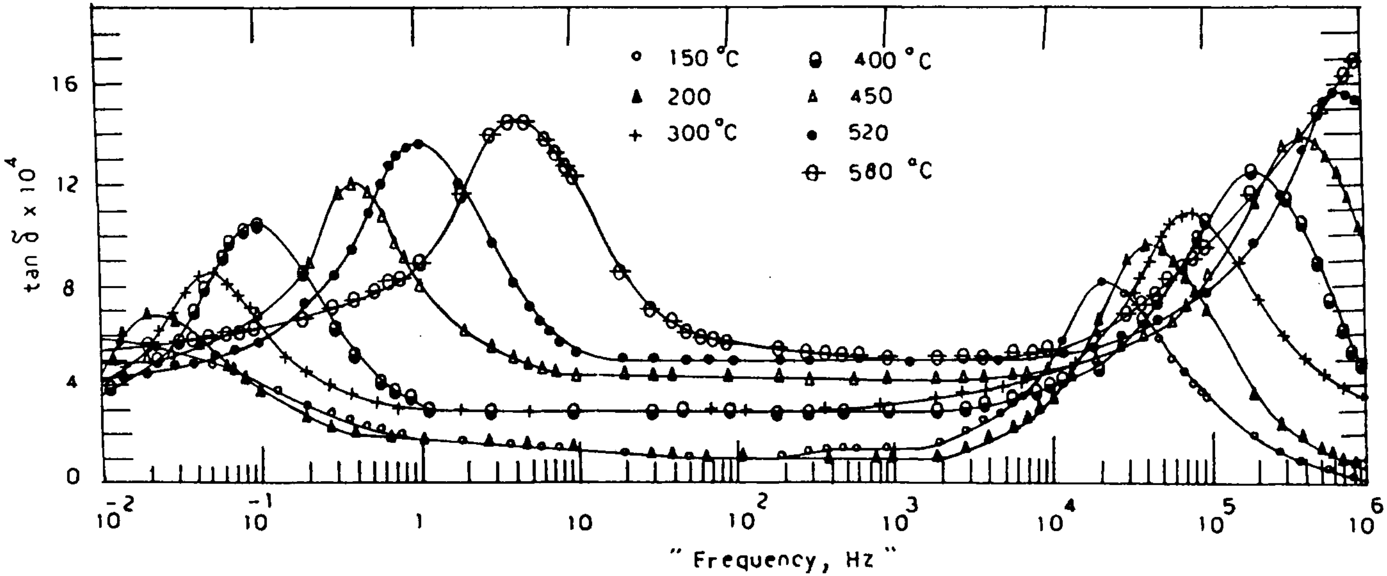

FIGURE 3 The frequency dependence of the loss angle δ at different temperatures.

values ε_∞ and ε_s, and having its center lying below the abscissa axis, where ε_s and ε_∞ are the static and optical dielectric constants.

The diameter drawn through the centre from the ε_∞ makes an angle $\alpha\pi/2$ with ε' axis. Tan $\alpha\pi/2$ is determined from the plots and α is calculated. Knowing α, one can determine the macroscopic relaxation time τ_0 by using the relation[7]

$$\frac{V}{U} = (\omega\tau_0)^{1-\alpha} \tag{1}$$

where V is the distance on the Cole–Cole diagram between ε_s and the experimental point, U is the distance between that point and ε_∞ and ω is the angular frequency. The parameter α is equal to zero when the dielectric has only one relaxation time, whereas for a distribution of relaxation times α varies between 0 and 1. The larger α is, the larger is the extent of the distribution of relaxation times. Knowing τ_0, one can estimate the value of the molecular relaxation time (τ) using the relation[8]

$$\tau = \frac{\tau_0(2\varepsilon_s + \varepsilon_\infty)}{3\varepsilon_s} \tag{2}$$

Cole–Cole diagrams for different temperatures are shown in Figure 4 and the calculated values of ε_s, ε_∞, α, τ_0 and τ are indicated in Table I. The data show that the molecular relaxation time decreases with the temperature, while the static dielectric constant increases.

b) Thermodynamic Parameters

Eyring[9] had pointed out the possibility of approaching the dielectric relaxation from the standpoint of chemical rate theory. According to his theory,[10],[11] the molecular relaxation time is given by

$$\tau = \left(\frac{h}{kT}\right) \exp\left(\frac{\Delta F}{RT}\right) \tag{3}$$

where ΔF is the free energy of activation for dipole relaxation, k is Boltzmann's constant and h is Planck's constant. Therefore, the free energy of activation can be calculated from the relation

$$\Delta F(K \cdot \text{Joule/mole}) = 2.303\, RT \log\left(\frac{\tau T \cdot k}{h}\right) \tag{4}$$

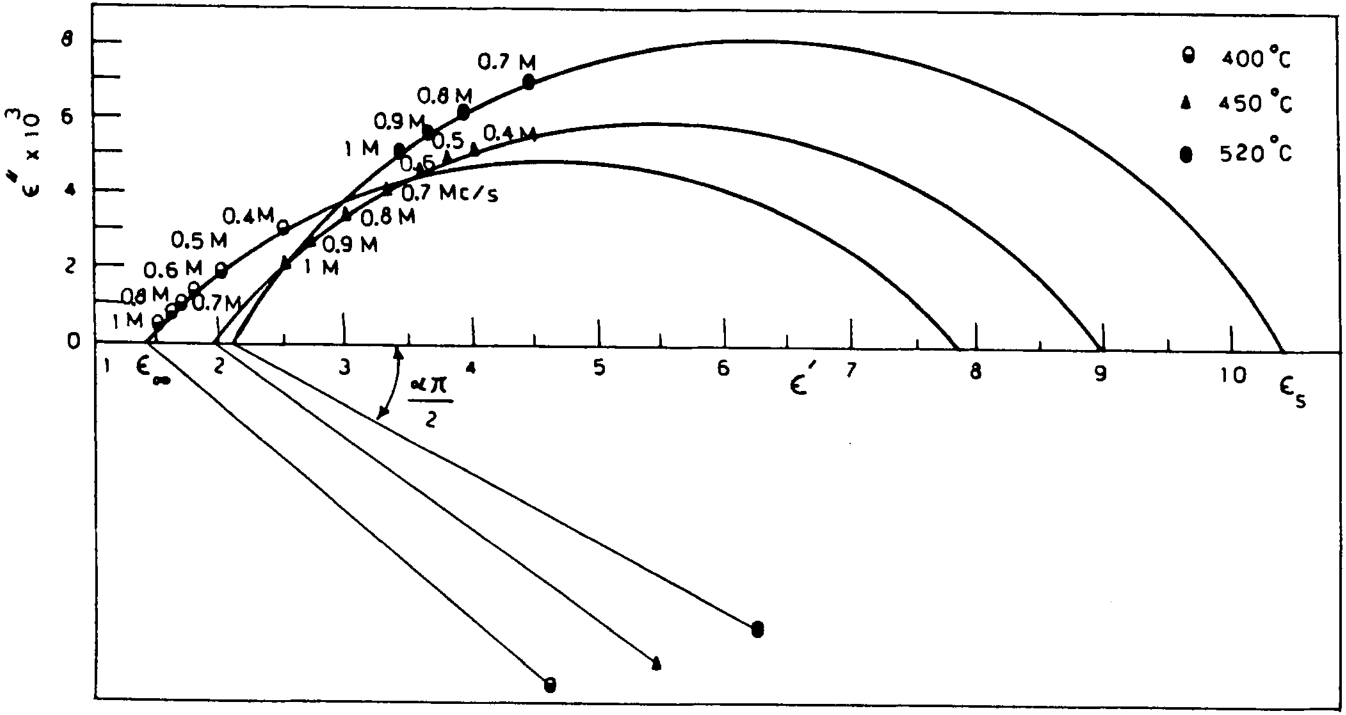

FIGURE 4 Cole–Cole plots at 400°C, 450°C and 520°C.

TABLE I

Temperature (°C)	ε_s	α	Macroscopic relaxation Time $\tau_0(s)$, Eq. (1)	Molecular relaxation time $\tau(s)$		Free energy of activation (K · Joule/mole) ΔF
				Cole–Cole, Eq. (2)	$\tau = 1/\omega_m$	
150	3.9	0.33	2.88×10^{-5}	22×10^{-6}	8×10^{-6}	63.64
200	4.0	0.36	1.06×10^{-5}	8.27×10^{-6}	3.4×10^{-6}	68.92
300	5.24	0.38	1.99×10^{-6}	4.9×10^{-6}	2.12×10^{-6}	81.39
400	7.92	0.46	7.96×10^{-7}	1.06×10^{-6}	0.8×10^{-6}	91.02
450	9.0	0.4	5.31×10^{-7}	1.21×10^{-6}	0.4×10^{-6}	94.04
520	10.46	0.31	2.27×10^{-7}	0.46×10^{-6}	0.23×10^{-6}	100.1
580					0.12×10^{-6}	103.58

The calculated values of ΔF at different temperatures are shown in Table I. The free energy of activation ΔF is related to the enthalpy of activation (ΔH) and the entropy of activation (ΔS) by

$$\Delta F = \Delta H - T\Delta S \tag{5}$$

From Eqs. (3) and (5) one obtains

$$2.303 \log\left(\frac{\tau T \cdot k}{h}\right) = \left(\frac{\Delta H}{RT}\right) - \frac{\Delta S}{R} \tag{6}$$

which indicate that the plot of $\log(\tau T)$ versus $1/T$ should give approximately a linear relation. Figures 5 and 6 show the plots of $\log(\tau T)$ vs. $1/T$ for the high frequency and low frequency loss peaks, the plots are linear, however, in the liquid state $\log(\tau T)$ decreases with temperature faster than in the solid state and a change of slope occurs near the melting point.

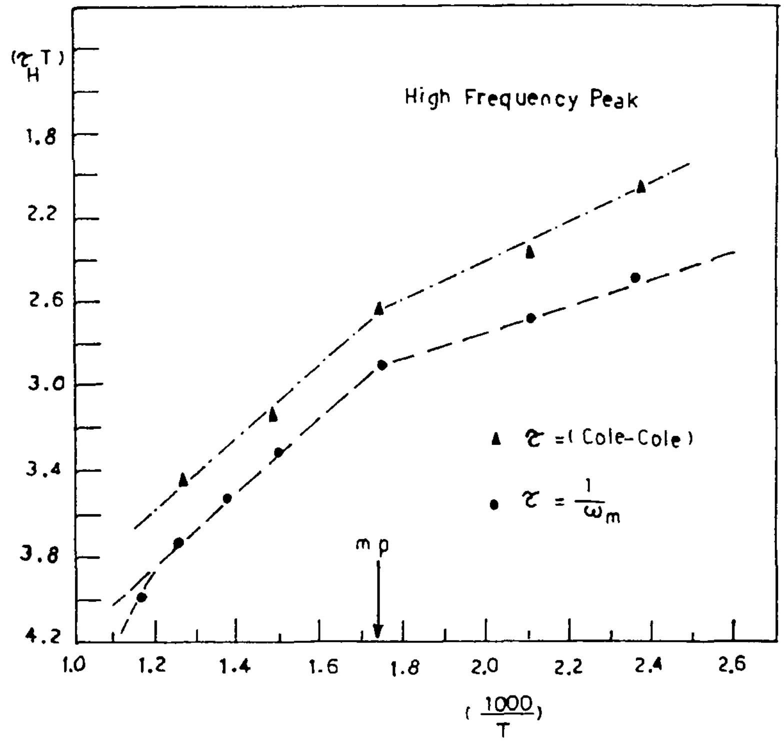

FIGURE 5 Temperature dependence of the molecular relaxation time for the high frequency dispersion peak:

▲ τ (Cole–Cole), ● $\tau = 1/\omega_m$

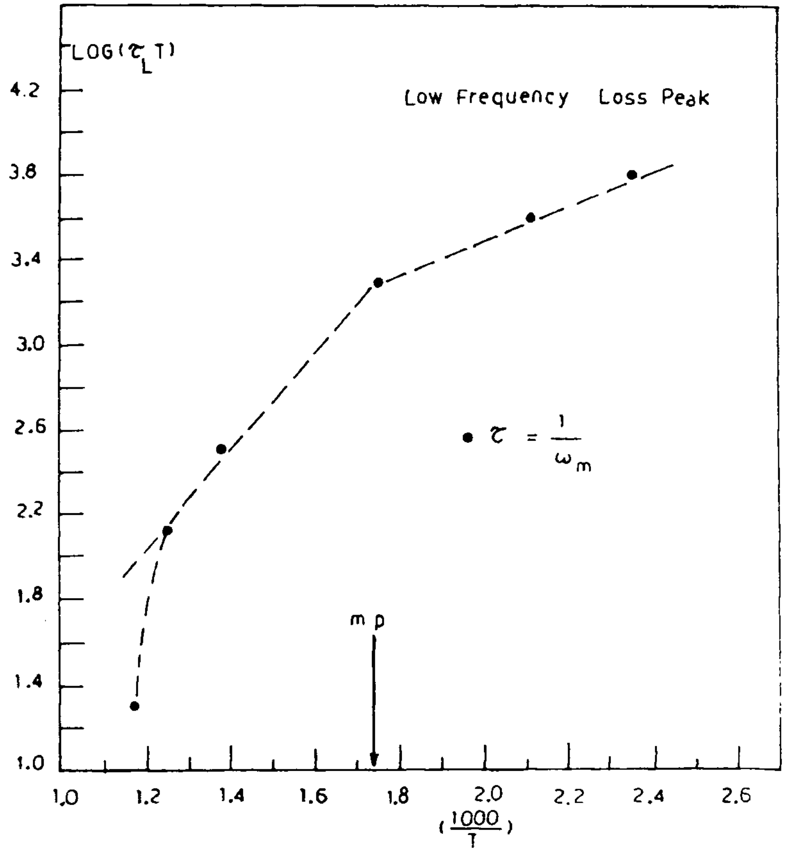

FIGURE 6 Temperature dependence of the molecular relaxation time for the low frequency dispersion peak.

4 DISCUSSION

Figures 2 and 3 show that the dielectric constant ε' and tan δ increases with the temperature, the rate of increase being different at different frequencies. This behaviour can be explained if we assume that the system exists in the form of molecular dipoles. As the temperature increases the dipoles slowly get activated and attain freedom of rotation, since the relative influence of the molecular interaction energy decreases with respect to that of thermal energy. According to Debye's concept[12] of viscosity dependence of relaxation time, and Eyring's (3), τ decreases exponentially with increasing temperature, which implies that ε' should increase exponentially with temperature. This is confirmed by plotting the curve log ε' versus $1/T$, which have been found to be linear for all frequencies as shown in Figure 7.

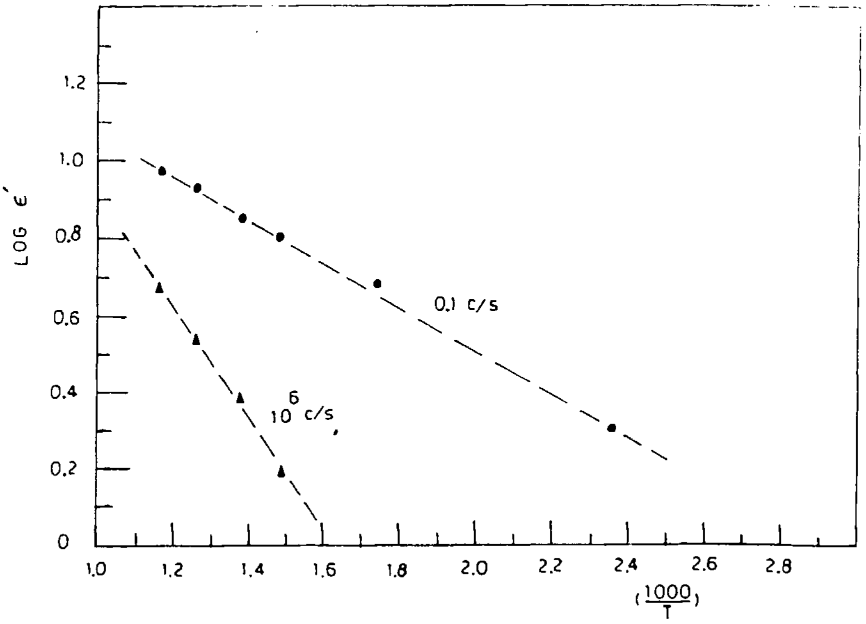

FIGURE 7 The temperature dependence of log ε' at different frequencies.

According to the Debye theory of intrinsic relaxation time the curves tan δ versus ω must be symmetrical. Figure 2 does reveal that the curves are nearly symmetrical around ω_m, where the angular frequency ω_m corresponds to maximum absorption,

$$\omega_m = \frac{1}{\tau} \tag{7}$$

where τ represents the most probable value of a spread of relaxation times. The values of τ calculated from Eq. 7 are inserted in Tables I and II. From Table I it is clear that there is a close proximity in the values of relaxation

TABLE II

Temperature (°C)	$\tau_L(s)$
150	15.92
200	7.96
300	3.18
400	1.59
450	0.40
520	0.17
580	0.035

times determined from Cole–Cole diagrams and those obtained by using Eq. 7. This is to be expected because both methods provide an average or most probable value of τ. Moreover, τ decreases with temperature, and the rate of decrease is faster in the liquid state than in the solid, which may be attributed to the effect of thermal energy, since it tends to weaken the forces of intermolecular interaction.

In general, dielectric relaxation does not follow exactly Debye's equation and is often represented by the Cole–Cole equation[7,13]

$$\varepsilon^* = \varepsilon_\infty + \frac{\Delta\varepsilon'}{1 + (j\omega\tau_0)^{1-\alpha})} \tag{8}$$

where $\Delta\varepsilon'$ is the magnitude of the dielectric dispersion. The height of the loss peaks should represent the density of the corresponding dipoles

$$(\tan\delta)_{\max} \propto \left(\frac{N\mu^2}{\varepsilon\varepsilon_0 kT}\right),$$

and the magnitude of the dielectric dispersion $\Delta\varepsilon'$ is proportional to the number of dipoles per unit volume

$$\Delta\varepsilon' \propto \left(\frac{N}{T}\right)$$

where μ is the dipole moment. Therefore, the observed increase in the height of the loss peak and the magnitude of dielectric dispersion with temperature suggests an increase in the density of the dipoles.

The measured dielectric loss data for the high frequency loss peak can be adequately interpreted in terms of the theory developed by Elliott[16] for ac conductivity and dielectric loss in chalcogenide glasses. This theory is based on charged defect concept suggested by Mott, Davis and Street,[14,15] in which dangling bonds can exist in paired states ($D^+ + D^-$) and are responsible for the density of states in the gap pinning the Fermi level. Elliott's theory[16] considers hopping of carriers between two sites over a barrier separating them, and the distribution of relaxation times for this process arises from the exponential dependence of the relaxation time on the barrier height. The hopping species was considered to be the doubly-occupied bipolaron state,[15,17] and the defect states were assumed to be sufficiently close (intimate valence alternation pairs)[17] that appreciable interaction occurs, thereby giving rise to a distribution of barrier heights separating them. Carriers are ejected from a D^- site into one of the excited levels and then drop into D^+ centre, converting it to a D^-. The theory predicts a dielectric loss peak when $\omega\tau_{\max} \simeq 1$, and the ac conductivity is given by the formula[16]

$$\sigma(\omega) = \frac{\pi^2 N^2 \varepsilon'}{24}\left(\frac{8e^2}{\varepsilon' W_M}\right)^6\left(\frac{\omega^s}{\tau_0^\beta}\right) \tag{9}$$

where W_M is the energy required to take two electrons from the D^- state to the continuum (the conduction band) in the absence of a nearby D^+ centre, τ_0 is the effective relaxation time, N is the concentration of localized sites, ε' is the bulk dielectric constant, $\beta = 6kT/W_M$ and $s = 1 - \beta$. According to the theory the ac conductivity has a slightly sublinear frequency dependence and W_M is given by

$$W_M = B - W_1 + W_2 \tag{10}$$

where B is the band gap of the material, and W_1 and W_2 are approximately the distortion energies associated with the neutral D^0 and D^+ states respectively. Following Elliott's assumption[16] that $W_1 = W_2$ as a first approximation, then $W_M = B$.

Equation 9 can be used to calculate the density of defects N, using the experimental values of ε', ω, T, τ_0 and $\sigma(\omega)$, where the ac conductivity was calculated directly from the experimental data using the formula[18]

$$\sigma_{\mathrm{ac}}(\omega) = \left(\frac{\omega C \tan\delta}{1 + (\tan\delta)^2}\right)\frac{l}{A}(1 - 2\tan\delta D_0)$$

where C is the sample capacitance, l/A is the geometric factor, D_0 is a correction factor.[18] Table III gives representative data for the estimated values of N calculated at different temperatures and at loss peak $(\tan\delta)_{\max}$. From Table III it is clear that the density of defects N increases with the temperature, moreover, the deduced values of the spatial density of defects N are similar in magnitude with estimates for other semiconductor materials Se, As_2Se_3 and As_2S_3 in the amorphous state.[16]

TABLE III

Temperature (°C)	N_{calc} (m^{-3})
150	2.81×10^{23}
200	2.5×10^{23}
300	8.42×10^{23}
400	2.94×10^{24}
450	3.2×10^{24}
520	4.2×10^{24}
580	6.77×10^{24}

Low Frequency Dispersion Peak

The frequency range of the low frequency loss peak (0.09 Hz to 4 Hz) indicates that this loss peak may be due to the space charge or interfacial polarization. The presence of heterogeneities in the sample which may be due to internal structural effects such as microscopic fluctuations in density will act as a physical barrier that inhibits charge migration and charges pile up at the barrier producing a localized polarization of the material. Moreover, electrode polarization characterized by accumulation of charge carriers onto the electrodes, can be responsible for dielectric loss peaks. However, easy saturation of the relevant polarization at higher frequencies than expected for electrode polarization leads us to assume that the low frequency loss peak may be due to jumping of charge carriers from one site to some nearest-neighbor site in the direction of the applied field over the potential barrier.

5 CONCLUSIONS

Dielectric loss in ternary amorphous and liquid semiconductor $AgTlSe_2$ was adequately interpreted using the charged defect D^+D^- model, where two electrons hopping is responsible for the ac conductivity mechanism. The density of defects was found to increase with temperature, which explains the increase of $(\tan\delta)_{max}$ and $\Delta\varepsilon'$ with temperature.

References

1. N. F. Mott, *Phil. Mag.*, **13**, 989 (1966); **24**, 1 (1971).
2. N. F. Mott and E. A. Davis, *Electronic Processes in Non-Crystaline Materials*, Clarendon Press Oxford 1971.
3. H. Fritzsche, *Amorphous and Liquid Semiconductors*. Ed. J. Tauc, Plenum Press, New York 1974, p. 221.
4. M. Cutler, *Liquid Semiconductors*, Academic Press, New York 1977.
5. V. P. Zhuze, V. P. Sergeeva, and E. L. Shtrum, *Sov. Phys. Tech. Phys.*, vol. 3, No. 10. 1925 (1958).
6. J. L. Shay and J. M. Wernick, *Ternary Chalcopyrite Semiconductors*, Pergamon Press, Oxford 1975.
7. R. H. Cole and R. S. Cole, *J. Chem. Phys.*, **9**, 341 (1941).
8. J. G. Powles, *J. Chem. Phys.*, **21**, 633 (1953).
9. H. Eyring, *J. Chem. Phys.*, **4**, 283 (1936).
10. A. E. Stearn and H. Eyring, *J. Chem. Phys.*, **5**, 113 (1937).
11. S. Glasstone, K. J. Laidler, and H. Eyring, *The Theory of Rate Processes*, McGraw-Hill, New York, 1941, p. 544.
12. P. Debye, *Polar Molecules*, New York (1929).
13. M. Tomozawa, *J. Non-Crystalline Solids*, **33**, 117 (1979).
14. N. F. Mott, E. A. Davis, and R. A. Street, *Phil. Mag.*, **32**, 961 (1975).
15. R. A. Street and N. F. Mott, *Phys. Rev. Letters*, **35**, 1293 (1975).
16. S. R. Elliott, *Phil. Mag.*, **36**, 1291 (1977).
17. M. Kastner, D. Adler, and H. Fritzsche, *Phys. Rev. Lett.*, **37**, 1504 (1976).
18. M. Pollak and T. H. Geballe, *Phys. Rev.*, **22**, 6, 1742 (1961).